whereas the trustee is wholly dependent on the investor's cooperation. This dependency of the trustee on the investor likely results in greater responsivity by the trustee to changes in investor reciprocity.
21. A description of methods is available as supporting material in *Science* Online.
22. Each dyad contributed eight behavioral events to this analysis (48 pairs × 8 rounds = 384 rounds). Investor reciprocity cannot be calculated for the initial two rounds and was excluded. The 384 rounds had a mean ± SD of −0.01 ± 0.35, skewness of −0.19 (SE = 0.12), and kurtosis of 2.55 (SE = 0.25). Rounds were divided into approximately equal-sized categories: 125 malevolent reciprocity rounds ($x < -0.025$), 134 neutral reciprocity rounds ($-0.025 \leq x \leq +0.05$), and 125 benevolent reciprocity rounds ($x > +0.05$). For additional description of reciprocity categories, see figs. S3 and S4.
23. Regions with ≥10 significant voxels were identified using *t* tests. *Z* values and statistical parametric mapping (SPM) coordinates for each region are available in table S1.
24. The correlation of change in investment (ΔI_j) and subsequent change in repayment (ΔR_j) grew as experience between players accrued (fig. S5).
25. P. Dayan, L. F. Abbott, *Theoretical Neuroscience* (MIT Press, Cambridge, MA, 2001).
26. K. C. Berridge, in *The Psychology of Learning and Motivation*, D. L. Medin, Ed. (Academic Press, New York, 2000), pp. 223–278.
27. A. Dickinson, B. W. Balleine, in *Steven's Handbook of Experimental Psychology*, C. R. Gallistel, Ed. (Wiley, New York, 2002), vol. 3, pp. 26–72.
28. G. Pagnoni, C. F. Zink, P. R. Montague, G. S. Berns, *Nat. Neurosci.* **5**, 97 (2002).
29. S. M. McClure, G. S. Berns, P. R. Montague, *Neuron* **38**, 339 (2003).
30. J. P. O'Doherty, P. Dayan, K. Friston, H. Critchley, R. J. Dolan, *Neuron* **38**, 329 (2003).
31. J. O'Doherty *et al.*, *Science* **304**, 452 (2004).
32. B. Seymour *et al.*, *Nature* **429**, 664 (2004).
33. W. Schultz, P. Dayan, P. R. Montague, *Science* **275**, 1593 (1997).
34. P. R. Montague, S. E. Hyman, J. D. Cohen, *Nature* **431**, 760 (2004).
35. R. C. O'Reilly, T. S. Braver, J. D. Cohen, in *Models of Working Memory: Mechanisms of Active Maintenance and Executive Control*, A. Miyake, P. Shah, Eds. (Cambridge Univ. Press, New York, 1999), chap. 11, pp. 375–411.
36. K.-H. Lee, T. F. D. Farrow, S. A. Spence, P. W. R. Woodruff, *Psychol. Med.* **34**, 391 (2004).
37. E. L. Hill, U. Frith, *Philos. Trans. R. Soc. London Ser. B* **358**, 281 (2003).
38. P. A. Johnson, R. A. Hurley, C. Benkelfat, S. C. Herpertz, K. H. Taber, *J. Neuropsychiatry Clin. Neurosci.* **15**, 397 (2003).
39. This work was supported by the Center for Theoretical Neuroscience at Baylor College of Medicine (P.R.M.), National Institute on Drug Abuse (NIDA) grant DA11723 (P.R.M.), National Institute of Neurological Disorders and Stroke grant NS045790 (P.R.M.), National Institute of Mental Health grant MH52797 (P.R.M.), NIDA grant DA14883 (G. Berns), The Kane Family Foundation (P.R.M.), The David and Lucile Packard Foundation (S.R.Q.), and The Gordon and Betty Moore Foundation (S.R.Q.). We thank P. Dayan, J. Li, T. Lohrenz, C. Stetson, and two anonymous referees for comments on this manuscript. We thank the Hyperscan Development Team at Baylor College of Medicine for Network Experiment Management Object (NEMO) software implementation (www.hnl.bcm.tmc.edu/nemo) and G. Berns for early discussions and efforts leading to the development of hyperscanning. We also thank A. Harvey, S. Flaherty, K. Pfeiffer, R. Pruitt, and S. Gleason for technical assistance.

Supporting Online Material
www.sciencemag.org/cgi/content/full/308/5718/78/DC1
Materials and Methods
Figs. S1 to S6
Table S1
References

30 November 2004; accepted 7 February 2005
10.1126/science.1108062

Postsynaptic Receptor Trafficking Underlying a Form of Associative Learning

Simon Rumpel,[1] Joseph LeDoux,[2] Anthony Zador,[1] Roberto Malinow[1]*

To elucidate molecular, cellular, and circuit changes that occur in the brain during learning, we investigated the role of a glutamate receptor subtype in fear conditioning. In this form of learning, animals associate two stimuli, such as a tone and a shock. Here we report that fear conditioning drives AMPA-type glutamate receptors into the synapse of a large fraction of postsynaptic neurons in the lateral amygdala, a brain structure essential for this learning process. Furthermore, memory was reduced if AMPA receptor synaptic incorporation was blocked in as few as 10 to 20% of lateral amygdala neurons. Thus, the encoding of memories in the lateral amygdala is mediated by AMPA receptor trafficking, is widely distributed, and displays little redundancy.

Animals continually adapt their behavior in response to changes in the environment. It has long been held that selective modifications in synaptic efficacy represent the physical substrate for this behavioral plasticity (*1*, *2*). Long-term potentiation (LTP), a cellular model of synaptic plasticity, has emerged as a leading candidate mechanism underlying associative forms of learning in the central nervous system (*3*–*12*). Much is now known about the molecular mechanisms during LTP that translate a brief change in electrical activity patterns to a modification in synaptic efficacy (*13*–*23*). Recent studies indicate that synaptic addition of GluR1 subunit–containing AMPA-type glutamate receptors (GluR1-receptors) mediates the synaptic strengthening observed during LTP (*24*, *25*). An attractive

[1]Cold Spring Harbor Laboratory, Cold Spring Harbor, NY 11724, USA. [2]New York University, New York, NY 10003, USA.

*To whom correspondence should be addressed. E-mail: malinow@cshl.edu

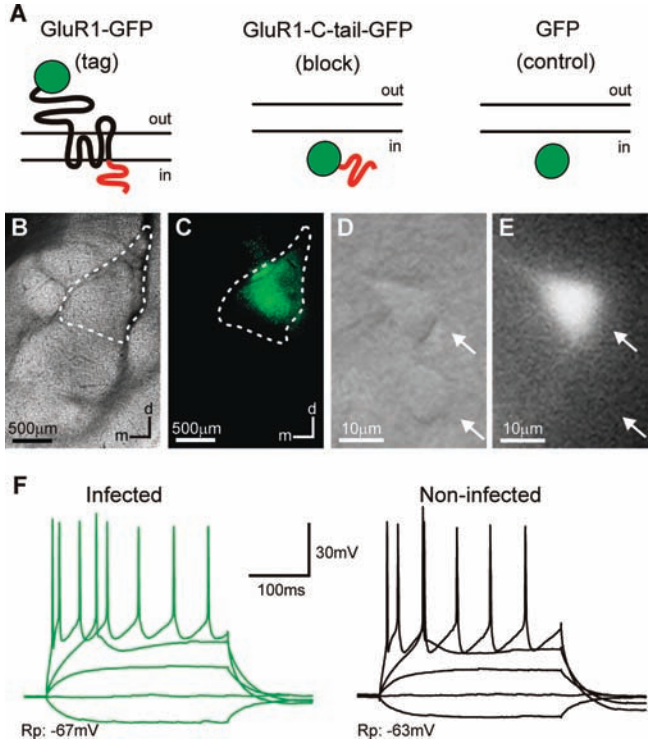

Fig. 1. Viral infection with amplicon vectors does not alter basic electrophysiological properties. (**A**) Schematic of recombinant proteins used in this study: GluR1-GFP, a fusion protein of GFP and the GluR1 subunit; GluR1-C-tail–GFP, a fusion protein of GFP and the last C-terminal 81 amino acids of the GluR1 subunit; and GFP alone. (**B** and **C**) Low magnification transmitted light (B) and epifluorescence (C) images of a coronal section of the right hemisphere including the amygdala. Note the area of GFP-expressing cells within the lateral amygdala (dotted line) 1 day after injection. d, dorsal; m, medial. (**D** and **E**) Highly magnified image of the lateral amygdala by infrared-differential interference contrast microscopy (D) and epifluorescence (E), which contains a neuron expressing (upper arrow) or not expressing (lower arrow) GFP. (**F**) Superimposed current-clamp recordings of an infected (green traces) and noninfected (black traces) neuron during 300-ms current injections of −100, 0, +100, +200, and +550pA. Rp, resting potential of neurons indicated next to traces.

proposal is that a learning-driven increase in GluR1-receptors at a selected group of synapses underlies associative memory.

We tested this proposal by using auditory fear conditioning, a well-characterized behavioral paradigm in which an animal learns to associate a tone with an electric shock and subsequently "freezes" when presented with a tone alone (*11*, *12*, *26*). The memory formed by fear conditioning is long lasting and can be easily assessed. Lesions and pharmacological treatments indicate a role of the amygdala in acquisition and storage of fear memory traces. Furthermore, LTP occurs at the synapses between the auditory thalamus to the lateral amygdala in vitro and in vivo. We have therefore studied the role of GluR1-receptor trafficking at thalamo-amygdala synapses in associative fear conditioning.

Amplicon vectors to tag or block plasticity. To investigate the role of GluR1-receptor trafficking in fear conditioning, we used an acute gene delivery technique to express recombinant proteins in a spatially and temporally controlled manner within a targeted brain region (*27*–*31*). In this way, we could monitor and perturb AMPAR trafficking. We injected amplicon vectors based on nonreplicating herpes simplex virus (*32*) into the lateral amygdala of juvenile rats (*33*) (Fig. 1A). Infected cells could be identified by amplicon-driven coexpression of the green fluorescent protein (GFP). Expression was rapid and robust, so that infected cells were clearly visible in amygdala brain slices prepared 24 hours after in vivo injection (Fig. 1, B through E). The basic electrophysiological properties of infected neurons, including input resistance and firing properties, were indistinguishable from those of noninfected control neurons (*34*) (Fig. 1F).

The first amplicon vector we used (Fig. 1A) encodes GluR1 fused with GFP. This vector drives expression of homomeric AMPARs that display greater rectification (i.e., a greater conductance when passing inward than outward current) than endogenous AMPARs (*35*). Synapses undergoing plasticity by incorporation of recombinant GluR1-receptors show increased rectification compared with synapses with only endogenous AMPARs. These receptors thus act as a "plasticity tag" for modified synapses that can be detected with an electrophysiological assay (*36*). The second amplicon vector encodes the carboxyl cytoplasmic tail (81 amino acids) of GluR1 fused with GFP. The resulting protein acts as a dominant-negative construct to prevent synaptic incorporation of endogenous GluR1-receptors and thereby blocks several forms of synaptic plasticity in vitro and in vivo (*36*, *37*); we designate this the "plasticity-block" vector. A third amplicon vector (the "infection-control" vector) drives expression of only GFP and serves as a control for infection.

There is little synaptic incorporation of GluR1-receptors in the absence of strong plasticity-inducing stimuli (*38*). We thus first assessed trafficking of GluR1-receptors in the lateral amygdala of animals that were not subjected to fear conditioning. We prepared brain slices from naïve animals 36 hours after in vivo infection of the lateral amygdala with the plasticity-tag vector. Rectification of AMPAR-mediated transmission between auditory thalamus and lateral amygdala (*11*) was similar in infected and noninfected neurons (Fig. 2, A to C), which indicated no detectable synaptic incorporation of recombinant GluR1-receptors in naïve rats. In a second series of experiments, we injected the plasticity-block

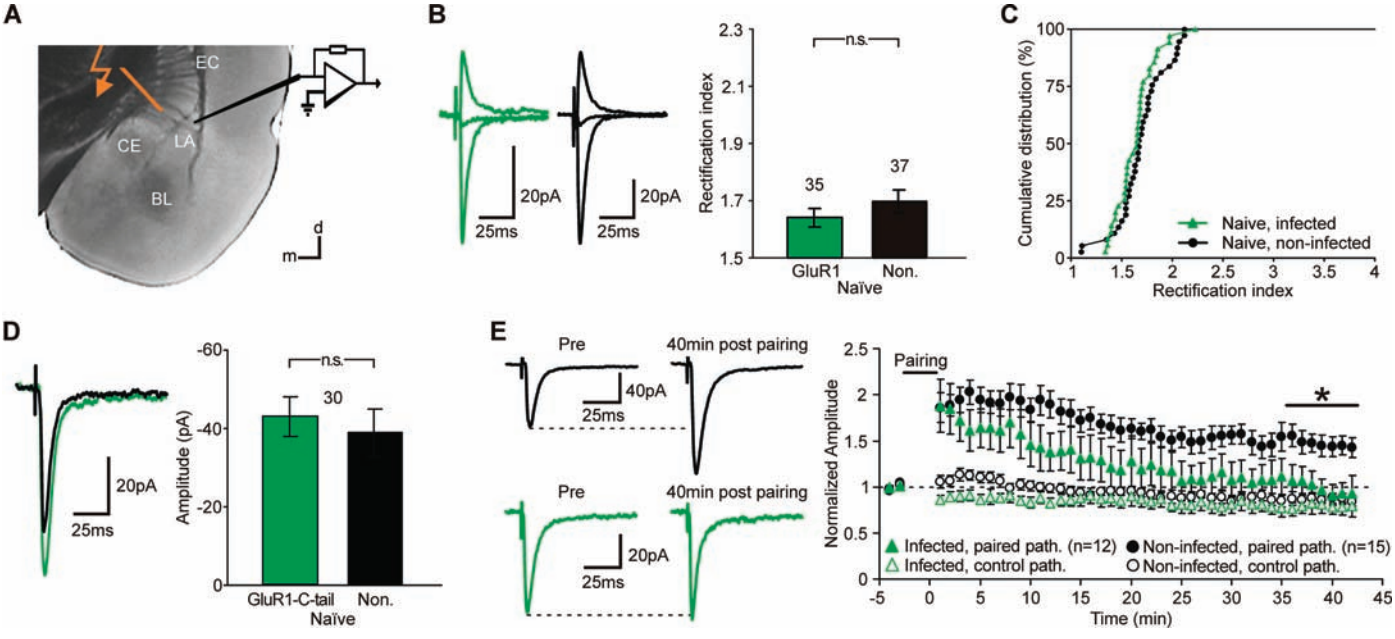

Fig. 2. Trafficking of GluR1 subunit–containing AMPARs in the lateral amygdala of naïve rats. (**A**) Transmitted light image of an acute amygdala slice preparation. Placement of stimulation and recording electrodes indicated. LA, lateral nucleus of the amygdala; BL, basolateral nucleus of the amygdala; CE, central nucleus of the amygdala; EC, external capsule; d, dorsal; m, medial. Note bundles of thalamo-amygdala fibers in the ventral striatum. (**B**) (Left) Evoked AMPAR-mediated postsynaptic currents (AMPA PSCs; 25 to 40 responses averaged) at –60, 0, and +40 mV holding potential recorded from a neuron infected with the plasticity-tag vector (green traces) and noninfected neuron (black traces). (Right) Mean rectification indices of synaptic pathways [RI, (amplitude at –60 mV holding potential)/(amplitude at +40 mV holding potential)] onto neurons infected with the plasticity-tag vector and noninfected neurons showed no statistically significant differences (*t* test, $P = 0.34$; n.s.), which suggests no incorporation of recombinant receptors in naïve animals. (**C**) Cumulative distribution plot of data shown in (B). (**D**) (Left) Superimposed averages (25 to 40 responses) of evoked AMPA PSCs recorded simultaneously in a neuron infected with the plasticity-block vector (green trace) and noninfected neuron (black trace) at –60 mV holding potential. (Right) Mean amplitude of evoked AMPA PSCs recorded simultaneously in pairs of neurons infected with the plasticity-block vector and not infected showed no statistically significant difference (*t* test, $P = 0.67$; n.s.). (**E**) (Left) Evoked AMPA PSCs (12 responses averaged) recorded in a noninfected neuron (black traces) and a neuron expressing plasticity-block vector (green traces) before and 40 min after LTP induction. (Right) Mean AMPA PSC amplitudes in neurons infected with the plasticity-block vector and noninfected neurons before and after the pairing protocol. Amplitudes were normalized to levels before pairing. Transmission in paired pathways from infected neurons returned to basal levels 40 min after LTP induction and was significantly lower than in paired pathways in control neurons (*t* test, $^*P < 0.01$). Error bars in this and all other figures are SEM.

vector into the lateral amygdala of rats to probe the trafficking of endogenous GluR1-receptors. Brain slices were prepared 14 to 20 hours after injection, to allow sufficient time to detect expression of the construct in neurons. The amplitude of basal AMPAR-mediated transmission was not affected by the plasticity-block construct, as assessed by simultaneous recordings of evoked transmission in nearby infected and noninfected neurons (Fig. 2D). Had there been synaptic incorporation of endogenous GluR1-receptors during the expression of the plasticity-block construct, synaptic currents would have been smaller in infected neurons (*39*). We then used the plasticity-block vector to assess the role of GluR1 trafficking during LTP in lateral amygdala neurons (Fig. 2E). In non-infected neurons, an LTP-inducing protocol led to persistent enhanced transmission. However, in neurons expressing the plasticity-block construct, the same stimulus protocol led only to a brief increase in transmission, similar to the results in hippocampus (*38*). Taken together, these results suggest that there was little or no synaptic incorporation of GluR1-receptors in the lateral amygdala of naïve rats during the expression period we examined.

Associative learning drives AMPARs into synapses. We next tested the first key prediction of the trafficking hypothesis: Conditioning should induce the incorporation of GluR1-receptors into thalamo-amygdala synapses. We injected the plasticity-tag vector into the lateral amygdala to monitor synapses undergoing plasticity. Thirty-six hours after injection, in one group of animals, we paired tones with shocks; in a second group, which

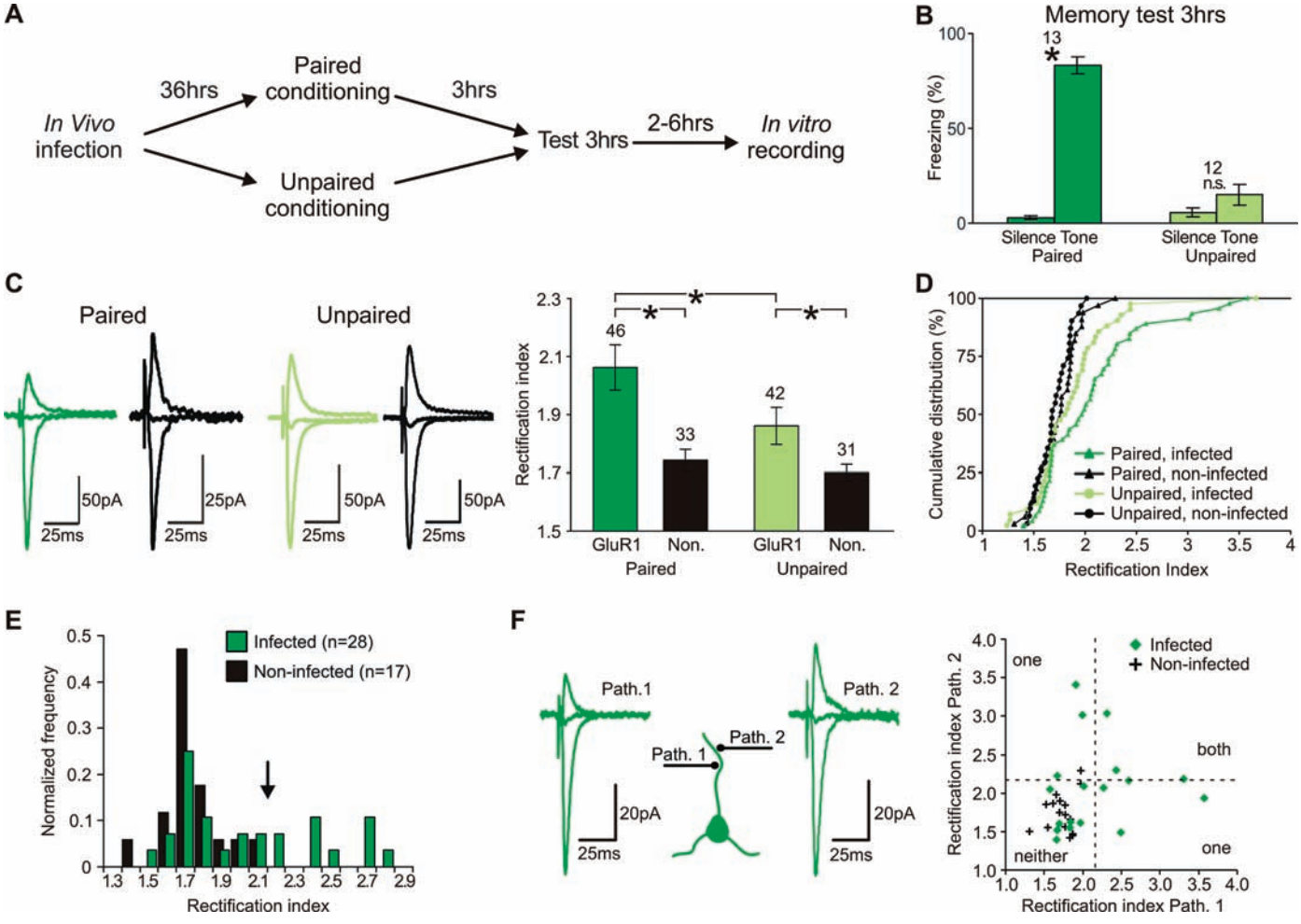

Fig. 3. Fear conditioning induces synaptic incorporation of recombinant GluR1 subunit–containing AMPA receptors. (**A**) Schematic of the experimental protocol. (**B**) Behavioral analysis of animals infected with the plasticity-tag vector 3 hours after either a paired conditioning protocol (solid green bars) or as control an unpaired conditioning protocol (hatched green bars). Freezing behavior was scored in testing cage during 1 min of silence and 1 min of tone presentation, as indicated. Animals from the paired group showed significantly increased freezing during tone presentation (*t* test, $*P < 0.01$). (**C**) (Left) Superimposed averages of evoked AMPA PSCs recorded at –60, 0, and +40 mV holding potential from neurons infected with the plasticity-tag vector (green) and noninfected (black) neurons from animals that underwent paired or unpaired conditioning. Note the strongly increased rectification in infected neuron from paired animal. (Right) Mean RIs of synaptic pathways from neurons infected with the plasticity-tag vector (GluR1) and noninfected neurons (non) from paired and unpaired animals (Paired, GluR1 versus non, *t* test, $P < 0.01$; unpaired, GluR1 versus non, *t* test, $P < 0.05$; GluR1, paired versus unpaired, *t* test, $P < 0.05$; significant differences indicated by asterisks). (**D**) Cumulative distribution of RIs from (C). Note the divergence of distributions for RI values >1.7. (**E**) Histogram of RIs in infected and noninfected neurons from paired animals (RIs have been averaged in case two synaptic pathways have been obtained from one neuron). Of tested lateral amygdala neurons, 36% showed learning-induced synaptic delivery of GluR1-receptors as estimated by determining the number of infected neurons that show RIs larger than two standard deviations of the distribution from noninfected neurons (arrow). (**F**) Learning-induced delivery of GluR1-receptors occurs at subsets of synapses and is not neuron-wide. (Left) Superimposed averages of evoked AMPA PSCs recorded at –60, 0, and +40 mV holding potential in a single neuron expressing the plasticity-tag construct. Two individual synaptic pathways onto the neuron had been probed by interleaved stimulation of two separate bundles of thalamo-amygdala fibers (see Fig. 2A). Note strong differences in rectification between pathways. (Right) Scatter plot of RIs from two pathways recorded in single neurons infected with the plasticity-tag vector (green diamonds) and single noninfected neurons (black crosses). RIs from pathways in infected neurons were not significantly correlated ($R^2 = 0.014$).

served as control for nonassociative learning, we delivered the same number of tones and shocks, but in an unpaired fashion (Fig. 3A). As expected (*11*, *12*), the paired group showed robust freezing in response to a test tone presented 3 hours later, whereas the unpaired control group did not (Fig. 3B). After behavioral testing, we prepared brain slices from both groups and examined synaptic transmission between auditory thalamus and lateral amygdala. In slices from each group, we measured rectification of transmission onto neurons expressing the plasticity-tag construct, as well as onto noninfected neurons.

Infected neurons from the paired group showed significantly more rectification than infected neurons from the unpaired group (Fig. 3, C and D), indicating synaptic delivery of GluR1-receptors during this form of associative learning. About 36% of infected neurons in the paired group displayed rectification values more than two standard deviations above the mean rectification of the noninfected cells (Fig. 3E). This suggests that about one-third of neurons in the lateral amygdala undergo plasticity after formation of the memory of the tone-shock pairing.

Rectification indices in infected neurons from unpaired animals were slightly but significantly higher than in noninfected neurons from unpaired animals (Fig. 3, C and D) and infected neurons from naïve animals (*t* test, $P < 0.01$) (Fig. 2, B and C). This result may be due to the occurrence of some forms of learning in the lateral amygdala (such as contextual learning, or learning that the tone predicts no shock) in the unpaired group that may drive GluR1-receptor incorporation but is not measured by our behavioral assay (*40*–*42*). In summary, our findings demonstrate that associative fear conditioning is a powerful stimulus for the incorporation of GluR1-receptors into synapses of auditory input to lateral amygdala neurons.

Learning-induced receptor trafficking is pathway-specific. One of the hallmarks of LTP is that it is pathway-specific: Only synapses that meet the conditions for induction undergo potentiation (*43*). We therefore examined whether learning-induced receptor trafficking in vivo occurred at all synapses onto a cell, or at only a subset of synapses. We compared rectification of two synaptic pathways onto infected lateral amygdala cells from the paired group. Synaptic responses were evoked by stimulation of two individual thalamo-amygdala fiber bundles (Fig. 3F). In general, rectification indices from two auditory thalamic pathways onto the same infected lateral amygdala cell showed no significant correlation ($R^2 = 0.014$). Most cells displaying plasticity showed significantly increased rectification in only one pathway (7 out of 10). These results indicate that receptor trafficking induced by fear conditioning can be restricted to a subset of synapses and is not a cellwide phenomenon.

Synaptic incorporation of AMPARs is necessary for learning. We next tested a second key prediction of the trafficking hypothesis: Synaptic delivery of endogenous GluR1-receptors is necessary to acquire the conditioned response. Our approach was to test whether molecular block of GluR1-receptor synaptic incorporation impaired memory formation. We first established a moderate conditioning protocol that did not saturate learning (Fig. 4A). We reasoned that such a protocol would increase our ability to detect an effect on learning if only a small fraction of neurons were infected. We also wished to avoid possible compensation of partial memory impairment by overtraining (*44*). To probe the role of GluR1-receptor delivery in fear memory formation, we infected one group of animals with the plasticity-block vector, the amplicon that showed no effect on basal transmission in naïve animals (Fig. 2D) but can block plasticity-induced synaptic delivery of GluR1-receptors (*38*) (Fig. 2E). A control group was infected with the infection-control vector (Fig. 4B). To maximize the number of lateral amygdala neurons infected, animals received robust bilateral injections (1 to 2 μl total per amygdala). After allowing 14 to 20 hours for expression of constructs, we exposed animals to the moderate conditioning protocol and then later tested them for the conditioned response as a measure of memory. To avoid possible bias, we performed injections and testing blindly (i.e., the experimenter did not know the identity of the injected vector).

In memory retention tests 3 or 24 hours after training, animals that received robust injections of the plasticity-block vector showed significantly less freezing in response to the tone than did the group that received robust injections of the infection-control vector (Fig. 4C). This finding suggests impairment of fear acquisition that led to disruption of both short-term (3-hour) and long-term (24-hour) memory of the conditioning experience. During the conditioning protocol, the two groups of animals showed similar levels of freezing after the footshock. Since lesions of the amygdala disrupt postshock freezing (*11*), the differences in learning and the consequent effects on memory cannot be explained by a simple impairment of basic sensorimotor systems as might be expected, for example, from impairment of normal synaptic transmission rather than of plasticity. Thus, blockade of synaptic GluR1-receptor incorporation in lateral amygdala neurons can disrupt the learning processes that led to the formation of a lasting form of associative memory.

Disabling plasticity in few neurons impairs learning. We wished to determine the fraction of neurons in the lateral amygdala that must exhibit plasticity in order to

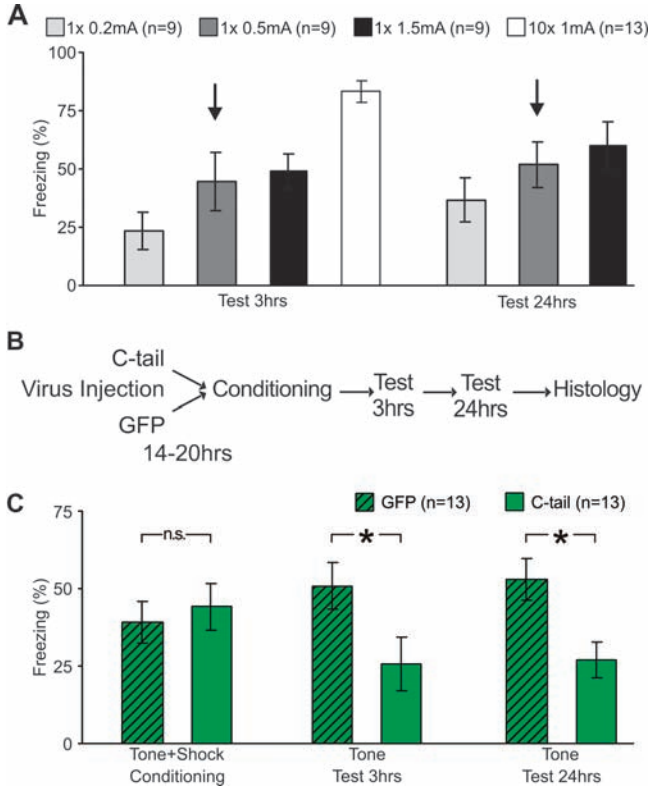

Fig. 4. Blocking synaptic incorporation of GluR1-receptors by overexpression of the plasticity-block construct impairs memory formation. (**A**) Behavioral analysis of noninfected animals 3 hours and 24 hours after single pairing of a tone and a footshock of varying intensity (protocols indicated). White bar illustrates freezing in animals conditioned with a protocol involving multiple pairing of tones and footshock (same data as Fig. 3B). The moderate conditioning protocol that was used in later experiments is indicated by arrows. (**B**) Schematic of the experimental protocol. (**C**) Behavioral analysis of animals infected either with the plasticity-block vector or the infection-control vector. Animals infected with the plasticity-block vector show significantly reduced freezing compared with control animals during memory retention tests (3 hours, *t* test, $P < 0.05$; 24 hours, *t* test, $P < 0.01$, significant differences indicated by asterisks), but not during the conditioning protocol (conditioning, *t* test, $P = 0.81$, n.s.).

support fear conditioning. We therefore used histological methods to estimate the proportion of neurons that were infected with the plasticity-block vector in the two lateral amygdalas of each animal (Fig. 5, A and B). After behavioral testing, the brain of each animal was removed, fixed, and sectioned serially, permitting three-dimensional analysis. For each brain section, we measured the fractional area of the lateral amygdala showing GFP fluorescence. By measuring fluorescence in all sections, the fraction of the two lateral amygdalas infected was calculated for each animal.

In order to estimate the fraction of infected neurons within each slice, we labeled several sections with a neuron-specific NeuN antibody (Fig. 5B). With dual-wavelength confocal imaging, individual neurons could readily be identified as infected or noninfected. The fraction of neurons displaying GFP in an infected region was measured [$\kappa = 0.58 \pm 0.04$ (mean ± SEM); $n = 5$ sections, two animals]. By multiplying this conversion factor κ by the fraction of the two lateral amygdalas infected, we could estimate the fraction of infected neurons in the two lateral amygdalas of each animal.

In animals that received robust injections with the plasticity-block vector, on average 27 ± 4% ($n = 13$) of lateral amygdala neurons were infected, indicating that blockade of synaptic GluR1 incorporation in as few as a quarter of neurons is sufficient to disrupt learning (Fig. 5C). We observed the same (27 ± 3%, $n = 13$) average rate of infection in control animals that received robust injections with the infection-control vector and showed normal learning, which indicated that expression of the plasticity-blocking construct, rather than variable infection levels, was responsible for the effect on learning.

Does abolishing plasticity in less than one-quarter of lateral amygdala neurons reduce learning? To obtain a lower bound on the fraction of lateral amygdala neurons required to produce an effect on learning, we tested an additional group of animals that received sparse bilateral infections of the plasticity-block vector or the infection-control vector (0.3 to 0.6 μl per amygdala). In these animals, the fraction of neurons infected was low (plasticity-block vector, 8 ± 1%, $n = 7$; infection-control vector, 7 ± 2%, $n = 6$; n.s.), and learning was normal (Fig. 5, C and D). Thus, if trafficking of GluR1-receptors is blocked in fewer than 10% of lateral amygdala neurons, then the animal displays normal learning. We pooled the data from the animals receiving robust and sparse infections and plotted the amount of freezing as a function of the fraction of infected neurons for each animal. We observed that most animals with 20% or more of lateral amygdala neurons infected with the plasticity-block vector showed diminished learning, whereas animals with less than 10% of neurons infected showed on average no effects on learning (Fig. 5E). Assuming that the amplicon vector does not preferentially infect neurons participating in encoding of the memory, these results indicate that blocking GluR1-receptor trafficking in ~10 to 20% of neurons undergoing plasticity is sufficient to impair memory formation in animals receiving moderate conditioning.

Cellular mechanisms of memory. We have shown that fear conditioning drives synaptic incorporation of GluR1-receptors in lateral amygdala neurons. It is noteworthy that not all synapses onto these plastic cells are modified, which suggests that learning-induced synaptic incorporation of GluR1-receptors is, like LTP, regulated in a synapse-specific manner. We find that interference with GluR1-receptor trafficking impairs amygdala LTP as well as fear conditioning, which indicates an essential contribution of this molecular process to memory formation. This view is supported by studies on genetically modified mice completely lacking the GluR1 subunit (*45*) that demonstrate impaired associative fear conditioning. Mice expressing GluR1 subunits with subtle mutations in phosphorylation sites (*46*) that block synaptic incorporation of recombinant GluR1-receptors (*47*) also show deficits in some associative forms of memory. Our findings establish the addition

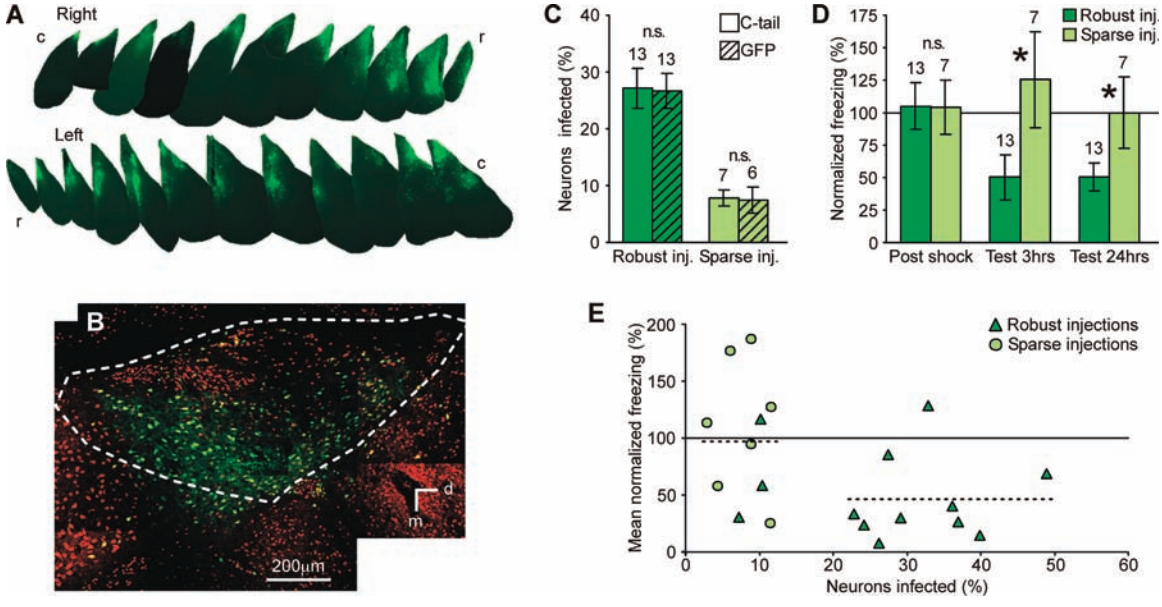

Fig. 5. Histological analysis of infection efficacy allows estimation of minimal fraction of plasticity-blocked neurons necessary to cause memory defects. (**A**) Montage of epifluorescence images of the lateral amygdala and basolateral nucleus of the amygdala taken from serial sections of the right (top) and left (bottom) hemisphere from an animal having received injections with the infection-control vector. r, rostral; c, caudal. (**B**) Combined dual-channel image of an injection site in the lateral amygdala by confocal laser scanning microscopy. Red channel, immunohistochemical labeling of neuronal marker NeuN; green channel, GFP expression from infected cells. Within the site of injection, 58% of neurons showed green fluorescence. Dotted line circumscribes lateral amygdala. d, dorsal; m, medial. (**C**) Fraction of amygdala neurons in animals infected with the plasticity-block vector (solid bars) and infection-control vector (hatched bars) for robust and intentionally sparse injections from a separate series of experiments; no statistically significant differences were observed between infection rate for the plasticity-block vector and the infection-control vector (robust, *t* test, $P = 0.92$; sparse, *t* test, $P = 0.89$, n.s.). (**D**) Behavioral analysis of animals with robust (same data as Fig. 4C) and sparse injections. Freezing of animals expressing the plasticity-block construct was normalized to control animals expressing only GFP. In memory retention tests, animals with sparse injections of the plasticity-block vector showed freezing levels similar to control animals and significantly higher freezing as animals with robust injections of the plasticity-block vector (3 hours, 24 hours, *t* test, $P < 0.05$, significant differences indicated by asterisks). (**E**) Freezing of animals expressing the plasticity-block construct was averaged across both test sessions, normalized to control animals, and plotted against the fraction of infected cells in the lateral amygdala [same data as in (D)]. Each symbol represents values from a single animal. Dotted lines indicate average freezing in animals with infection levels of 0 to 15% and 15 to 50%.

of postsynaptic receptors, as a form of synaptic plasticity, to be a key element in associative memory formation.

Circuit mechanisms of memory. By using molecular tagging techniques, we estimate that about a third of lateral amygdala neurons undergo plasticity during the formation of a memory driven by a single conditioning block. Because not all synapses on a plastic neuron undergo modification, one neuron may potentially participate in many memories, which allows combinatorial storage of a large number of memories (*48*–*50*). Perturbing plasticity in a small fraction of lateral amygdala neurons appears to be sufficient to reduce memory function, which suggests little robustness or redundancy. Memory formation may require coordinated changes in synaptic strength, and perturbing a few plastic units may corrupt integrated function, much as the inability of a few violinists to change key properly can detectably offset a symphonic performance. Finding such sensitivity to small perturbation is striking given that large lesions (*51*) or advanced brain pathology (*52*) produce little disturbance of memory formation.

References and Notes

1. S. Freud, in *The Origins of Psychoanalysis*, M. Bonaparte, A. Freud, E. Kris, Eds. (Basic Books, New York, 1895), pp. 356–359.
2. D. O. Hebb, *Organization of Behavior* (Wiley, New York, 1949).
3. M. S. Rioult-Pedotti, D. Friedman, J. P. Donoghue, *Science* **290**, 533 (2000).
4. P. Andersen, *Philos. Trans. R. Soc. London B Biol. Sci.* **358**, 613 (2003).
5. G. Lynch, *Philos. Trans. R. Soc. London B Biol. Sci.* **358**, 625 (2003).
6. B. L. McNaughton, *Philos. Trans. R. Soc. London B Biol. Sci.* **358**, 629 (2003).
7. R. G. Morris, *Philos. Trans. R. Soc. London B Biol. Sci.* **358**, 643 (2003).
8. S. Tonegawa, K. Nakazawa, M. A. Wilson, *Philos. Trans. R. Soc. London B Biol. Sci.* **358**, 787 (2003).
9. J. Lisman, *Philos. Trans. R. Soc. London B Biol. Sci.* **358**, 829 (2003).
10. H. Eichenbaum, *Neuron* **44**, 109 (2004).
11. J. E. LeDoux, *Annu. Rev. Neurosci.* **23**, 155 (2000).
12. S. Maren, *Annu. Rev. Neurosci.* **24**, 897 (2001).
13. R. A. Nicoll, *Philos. Trans. R. Soc. London B Biol. Sci.* **358**, 721 (2003).
14. G. L. Collingridge, J. T. Isaac, Y. T. Wang, *Nature Rev. Neurosci.* **5**, 952 (2004).
15. R. C. Malenka, M. F. Bear, *Neuron* **44**, 5 (2004).
16. R. Malinow, *Philos. Trans. R. Soc. London B Biol. Sci.* **358**, 707 (2003).
17. M. Sheng, M. J. Kim, *Science* **298**, 776 (2002).
18. I. Song, R. L. Huganir, *Trends Neurosci.* **25**, 578 (2002).
19. D. Johnston *et al.*, *Philos. Trans. R. Soc. London B Biol. Sci.* **358**, 667 (2003).
20. K. M. Harris, J. C. Fiala, L. Ostroff, *Philos. Trans. R. Soc. London B Biol. Sci.* **358**, 745 (2003).
21. C. Pittenger, E. R. Kandel, *Philos. Trans. R. Soc. London B Biol. Sci.* **358**, 757 (2003).
22. S. Choi, J. Klingauf, R. W. Tsien, *Philos. Trans. R. Soc. London B Biol. Sci.* **358**, 695 (2003).
23. D. Zamanillo *et al.*, *Science* **284**, 1805 (1999).
24. Y. Hayashi *et al.*, *Science* **287**, 2262 (2000).
25. M. Passafaro, V. Piech, M. Sheng, *Nature Neurosci.* **4**, 917 (2001).
26. C. F. Stevens, *Neuron* **20**, 1 (1998).
27. W. A. Carlezon Jr. *et al.*, *Science* **277**, 812 (1997).
28. A. Bahi, F. Boyer, T. Kafri, J. L. Dreyer, *Eur. J. Neurosci.* **19**, 1621 (2004).
29. Z. Dong *et al.*, *Proc. Natl. Acad. Sci. U.S.A.* **100**, 12438 (2003).
30. J. R. Goss *et al.*, *Methods Mol. Biol.* **246**, 309 (2004).
31. V. M. Sandler *et al.*, *J. Neurosci. Methods* **121**, 211 (2002).
32. R. L. Neve, A. I. Geller, *Adv. Neurol.* **79**, 1027 (1999).
33. S. A. Josselyn *et al.*, *J. Neurosci.* **21**, 2404 (2001).
34. E. S. Faber, R. J. Callister, P. Sah, *J. Neurophysiol.* **85**, 714 (2001).
35. J. Boulter *et al.*, *Science* **249**, 1033 (1990).
36. R. Malinow, R. C. Malenka, *Annu. Rev. Neurosci.* **25**, 103 (2002).
37. A. J. Watt, P. J. Sjostrom, M. Hausser, S. B. Nelson, G. G. Turrigiano, *Nature Neurosci.* **7**, 518 (2004).
38. S. Shi, Y. Hayashi, J. A. Esteban, R. Malinow, *Cell* **105**, 331 (2001).
39. T. Takahashi, K. Svoboda, R. Malinow, *Science* **299**, 1585 (2003).
40. K. A. Goosens, S. Maren, *Learn. Mem.* **8**, 148 (2001).
41. C. B. Sananes, M. Davis, *Behav. Neurosci.* **106**, 72 (1992).
42. P. S. Bellgowan, F. J. Helmstetter, *Behav. Neurosci.* **110**, 727 (1996).
43. P. Andersen, S. H. Sundberg, O. Sveen, H. Wigstrom, *Nature* **266**, 736 (1977).
44. S. Maren, *Eur. J. Neurosci.* **12**, 4047 (2000).
45. M. A. Good, A. Johnson, D. Bannerman, N. Rawlins, R. Sprengel, paper presented at the Annual Meeting of the Society for Neuroscience, San Diego, 23 to 27 October 2004.
46. H. K. Lee *et al.*, *Cell* **112**, 631 (2003).
47. J. A. Esteban *et al.*, *Nature Neurosci.* **6**, 136 (2003).
48. D. Marr, *Philos. Trans. R. Soc. London B Biol. Sci.* **262**, 23 (1971).
49. P. Andersen, M. Trommald, *J. Neurobiol.* **26**, 396 (1995).
50. M. B. Moser, E. I. Moser, *J. Neurosci.* **18**, 7535 (1998).
51. M. B. Moser, E. I. Moser, E. Forrest, P. Andersen, R. G. Morris, *Proc. Natl. Acad. Sci. U.S.A.* **92**, 9697 (1995).
52. D. A. Snowdon, *Ann. Intern. Med.* **139**, 450 (2003).

53. This project was supported by DFG Ru 900/2-1 (S.R.), NIH (J.L., A.Z., R.M.), Mathers Charitable Foundation and Sloane Foundation (A.Z.), and Ale Davis and Maxine Harrison Foundation (R.M.). We thank G. Di Cristo for help with confocal microscopy; R. Neve for help and materials for viral expression system; N. Dawkins-Pisany for technical assistance; R. Tsien, G. Buzsaki, J. Hopfield, and Z. Mainen for comments on an earlier version of this manuscript; and M. Moita for helpful discussions.

Supporting Online Material

www.sciencemag.org/cgi/content/full/1103944/DC1
Materials and Methods
Figs. S1 and S2
Reference and Notes

8 November 2004; accepted 8 February 2005
Published online 3 March 2005;
10.1126/science.1103944
Include this information when citing this paper.

REPORTS

Spin-Charge Separation and Localization in One Dimension

O. M. Auslaender,[1]* H. Steinberg,[1] A. Yacoby,[1]† Y. Tserkovnyak,[2] B. I. Halperin,[2] K. W. Baldwin,[3] L. N. Pfeiffer,[3] K. W. West[3]

We report on measurements of quantum many-body modes in ballistic wires and their dependence on Coulomb interactions, obtained by tunneling between two parallel wires in an GaAs/AlGaAs heterostructure while varying electron density. We observed two spin modes and one charge mode of the coupled wires and mapped the dispersion velocities of the modes down to a critical density, at which spontaneous localization was observed. Theoretical calculations of the charge velocity agree well with the data, although they also predict an additional charge mode that was not observed. The measured spin velocity was smaller than theoretically predicted.

Coulomb interactions have a profound effect on the behavior of electrons. The low-energy properties of interacting electronic systems are described by elementary excitations, which interact with each other only weakly. In two- and three-dimensional disordered metals, they are dubbed quasiparticles (*1*), as they bear a strong resemblance to free electrons (*2*), which are fermions carrying both charge and spin. However, the elementary excitations in one-dimensional (1D) metals, known as Luttinger liquids (*3*, *4*), are utterly different. Each is collective and highly correlated and carries either spin or charge.

We determined the dispersions of the elementary excitations in one dimension by measuring the tunneling current, I_T, across an

[1]Department of Condensed Matter Physics, Weizmann Institute of Science, Rehovot 76100, Israel. [2]Lyman Laboratory of Physics, Harvard University, Cambridge, MA 02138, USA. [3]Bell Labs, Lucent Technologies, 700 Mountain Avenue, Murray Hill, NJ 07974, USA.

*Present address: Geballe Laboratory for Advanced Materials, Stanford University, Stanford, CA 94305, USA.
†To whom correspondence should be addressed. E-mail: amir.yacoby@weizmann.ac.il

Science Supporting Online Material

Postsynaptic Receptor Trafficking Underlying a Form of Associative Learning

Rumpel, LeDoux, Zador and Malinow

Materials and Methods

Animals. Male or female adolescent Sprague-Dawley rats (postnatal day 20–25) were housed on a 12-hour light/dark cycle with *ad libitum* access to water and food. Procedures were performed in strict compliance with the animal use and care guidelines of Cold Spring Harbor Laboratory.

Infection of lateral amygdala neurons in vivo. Genes of interest (GFP; GFP fused to the N-terminus of the AMPA receptor subunit GluR1flop and GFP fused to the N-terminus of the C-terminal portion of the GluR1 subunit [(809–889); see (*S1*)] were cloned by using standard methods into a HSV-amplicon vector and verified by sequencing. Virus vectors were generated as described elsewhere (*S2, S3*). Animals were anaesthetized with Ketamine/Medetomidine (2 mg Ketamine HCl and 0.016 mg Medetomidine HCl / 50 g rat) and positioned in a stereotaxic apparatus. Injections of viral solutions (3–9 injection sites; 100–200 nl per injection) were delivered with a glass micropipette through a skull window (2–3 mm^2) by pressure application (5–12 psi, controlled by a Picrospritzer II, General Valve, Fairfield, NJ, USA). The injections were performed within the following stereotaxic coordinates: –2.2 mm to –3.9 mm from Bregma; 4.5 mm to 5.3 mm lateral from midline, and 5.7 mm vertical from cortical surface. Subsequently the skull and skin were repositioned and maintained with cyanacrylate glue. Infections with test or control vectors were delivered to animals from the same litter. During procedures, animals were kept on a heating pad and were brought back into their home cages after regaining movement. Animals infected with the plasticity-tag vector were kept in individual cages to avoid possible fearful experiences. Before behavioral training, we waited 14 to 20 hours for expression of cytosolic localized GluR1-C-tail-GFP and GFP and 36 hours for expression and processing of the membrane protein GluR1-GFP.

Electrophysiology. Animals were anesthetized with Ketamine/Medetomidine, decapitated and the brains quickly removed and chilled in ice-cold dissection buffer (110.0 mM choline chloride, 25.0 mM $NaHCO_3$, 1.25 mM NaH_2PO_4, 2.5 mM KCl, 0.5 mM $CaCl_2$, 7.0 mM $MgCl_2$, 25.0 mM glucose, 11.6 mM ascorbic acid, 3.1 mM pyruvic acid; gassed with 95%O_2/5%CO_2). Coronal slices (300 μm) were cut in dissection buffer using a VT-1000 S vibratome (Leica, Nussloch, Germany) and subsequently transferred to a storage chamber containing artifical cerebrospinal fluid (ACSF; 118 mM NaCl, 2.5 mM KCl, 26.2 mM $NaHCO_3$, 1 mM NaH_2PO_4, 20 mM Glucose, 4 mM $MgCl_2$, 4 mM $CaCl_2$; 22°–25°C; pH 7.4; gassed with 95%O_2/5%CO_2). After at least 1hr of recovery time slices were transferred to the recording chamber and were constantly perfused with ACSF maintained at 24°C. Patch-clamp whole-cell recordings of lateral amygdala neurons were obtained under IR-DIC visualization with Axopatch–1D amplifiers (Axon

Instruments, Foster City, CA). For basic voltage-clamp experiments we filled patch pipettes (3–6 MΩ) with 135 mM $CsMeSO_4$, 20 mM TEA-Cl, 2 mM $MgCl_2$, 10 mM Hepes, 10 mM EGTA, 5 mM QX-314, pH 7.25. In experiments investigating long-term synaptic plasticity we used 115 $CsMeSO_4$, 20 CsCl, 10 HEPES, 2.5 $MgCl_2$, 4 Na_2ATP, 0.4 Na_3GTP, 10 Na-phosphocreatine, 0.6 EGTA, pH 7.25. For current-clamp recordings pipettes were filled with 130 mM K-Gluconate, 5 mM KCl, 10 mM Hepes, 2.5 mM $MgCl_2$, 4 mM Na_2ATP, 0.4 mM Na_3GTP, 10 mM Na-phosphocreatine, 0.6 mM EGTA at pH 7.25. Liquid junction potential was not corrected.

We targeted large, pyramidal-like somata, thus selecting for spiny glutamatergic principal neurons, which make up the majority of neurons in the lateral amygdala. Firing patterns obtained in current-clamp recordings also have been consistent with previous data for principal neurons (*S4*). Synaptic responses were evoked by electrical stimulation of fibers in the ventral striatum just medial to the dorsal lateral amygdala with bipolar Platinum/Iridium electrodes (Frederick Haer & Co., Bowdoinham, ME). These fibers originate in the auditory thalamus and project to neurons in the lateral amygdala (*S5*). We reasoned that possible stimulation of fibers from sources other than the auditory thalamus would lead to an underestimation of learning-induced effects.

In experiments investigating synaptic incorporation of recombinant receptors AMPA receptor-mediated transmission was pharmacologically isolated by addition of 100 μM Picrotoxin and 50 μM D,L-AP5 to the ACSF. We recorded AMPA PSCs at –60, 0, and +40 mV holding potential and 25 to 40 consecutive responses from each holding potential were averaged. If possible, two synaptic pathways onto the same postsynaptic cell have been acquired by stimulation of two bundles of fibers in the ventral striatum. Half of the electrophysiological data from paired or unpaired rats was acquired and analyzed with the experimenter blinded to the protocol used for conditioning. No significant differences between blinded and non-blinded data were detected and therefore pooled.

In experiments analyzing long-term synaptic plasticity slices were maintained in ACSF with the following composition: 115 NaCl, 3.3 KCl, 25.5 $NaHCO_3$, 1.2 NaH_2PO_4, 5 lactic acid, 25 glucose, 1 $MgSO_4$, 2 $CaCl_2$, 100 μM Picrotoxin, equilibrated with 95% O_2/5% CO_2 (*S6*). In a subset of experiments (6 from 15 non-infected neurons; 4 from 12 infected neurons) standard ACSF was used as described above. In order to monitor synaptic transmission we evoked AMPA PSCs at two synaptic pathways by interleaved stimulation of two fiber bundles at 0.33 to 0.1Hz and recorded at –60 mV holding potential in voltage-clamp mode. LTP was induced at one pathway by a pairing protocol consisting of presynaptic fiber stimulation at 3Hz for 3 min paired with postsynaptic depolarization to 0 mV holding potential. Experiments were excluded from analysis if unpaired control pathways displayed changes in transmission by more than 50%.

All data were reported as mean ± SEM and significance level was set at $P<0.05$. Statistical differences were determined by unpaired two-tailed t-test for unpaired data or paired two-tailed t-test for paired data, unless otherwise stated. If necessary, data was log-normalized prior to testing.

Behavioral training and analysis. All animals were handled and habituated to the shocking chamber, testing chamber, and the conditional acoustic stimulus before entering

the experimental schedule. Conditioning was performed in a Habitest chamber (30 cm x 26 cm x 28 cm) with an electrifiable grid floor (Coulbourn Instruments, Allentown, PA) within a larger sound attenuated cabinet. During conditioning the cabinet was illuminated and the behavior was captured with an infrared PC-6EX2 CCD-camera (Supercircuits, Liberty Hill, Tx) and stored on a personal computer. Delivery of the shock and the tone was controlled by custom written software in Matlab (MathWorks, Natick, MA). Tones (either 0.5 s white noise bursts at 1Hz for 20 s at ~80 dB for HSV-GluR1 infected rats or 5kHz pure tones 20 s continuously at ~80 dB for the plasticity-block vector and the infection-control vector infected rats) were delivered via a RP2 real time processor (TDT, Alachua, FL) and a tweeter (Radio Shack, Fort Worth, TX) connected to a P1000 amplifier (Hafler, Tempe, Az). Each conditioning session was peformed with experimental and control animals in parallel. Conditioning with HSV-GluR1 infected animals was done with 10 tones, on randomized intervals, on average 3 min apart. In the paired group tones were co-terminated with a 0.5 s 1 mA footshock, in the unpaired group tones and shocks were separated by at least 1 min. Animals infected with the plasticity-block vector or the infection-control vector were conditioned with a single pairing of a tone, co-terminated with a 0.5 s 0.5 mA footshock. Memory retention tests were performed in darkness in a different shaped plastic container (20 cm x 20 cm x 28 cm) and behavior was recorded during 1 min of silence and 1 min of tone presentation. The fraction of time spent freezing (defined as complete cessation of all movements except breathing) was scored post hoc with the experimenter blinded to the vector that was used for infection.

Histology. After the last behavioral testing session all animals were anaesthetized, decapitated and the brains quickly chilled in ice-cold phosphate-buffered saline (PBS). The brains were trimmed to small blocks containing the amygdala and were subsequently immersion fixed in PBS containing 4% paraformaldehyde and 4% sucrose overnight at 4°C. After fixation 10–13 coronal slices (200 μm) containing the amygdala were cut and mounted on cover glasses. Transmitted light and epifluorescence images were taken from each section with a Spot CCD camera (Diagnostic Instruments, Sterling Heights, MI) mounted on an Axiophot microscope (Zeiss, Oberkochen, Germany). We focused our analysis on the lateral amygdala, as described by Paxinos and Watson (*S7*), because of its essential function in tone-cued fear conditioning (*S5, S8*). Therefore, we defined the lateral amygdala as an area of interest based on the transmitted light picture using custom written scripts in Matlab (MathWorks, Natick, MA). Based on the fluorescence images the fraction of pixels with fluorescence values higher than two standard deviations of background was calculated for all slices from each animal. This provided a measure for the area within the lateral amygdala that was infected for all animals.

In order to obtain an estimate of the fraction of neurons infected within a given lateral amygdala we furthermore needed to estimate the efficiency of infection at the level of individual cells within an area showing green fluorescence. Three slices from a GFP expressing and two slices from a GluR1-C-tail-GFP expressing animal were labeled immunohistochemically with a primary antibody against the neuron-specific nuclear marker protein NeuN (Chemicon, Temecula, CA) and a secondary antibody conjugated with fluorescent marker Alexa594 (Molecular Probes, Eugene, OR). GFP fluorescence differed markedly between randomly chosen somata within the area of injection and showed a clearly bimodal distribution, thus indicating a good discrimination between

infected and non-infected neurons. We found that within an infection site on average 58% of the NeuN-labeled neurons showed GFP fluorescence (range: 48–67%). Thus, the value obtained for fraction of infected area was multiplied by 0.58 to establish the fraction of infected neurons in the lateral amygdala.

Supplemental Figure S1:

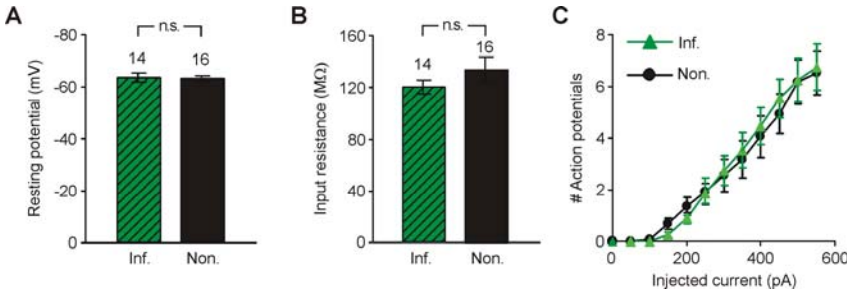

Fig. S1: Viral infection with amplicon vectors does not alter basic electrophysiological properties. Mean resting potential (*t* test, $P = 0.88$) (**A**), mean input resistance (*t* test, $P = 0.18$) (**B**), and input/output relationship (KS test, $P = 0.99$) (**C**) of infected (green bars) and non-infected (black bars) neurons showed no statistically significant differences (n.s.). Error bars are SEM.

Supplemental Figure S2:

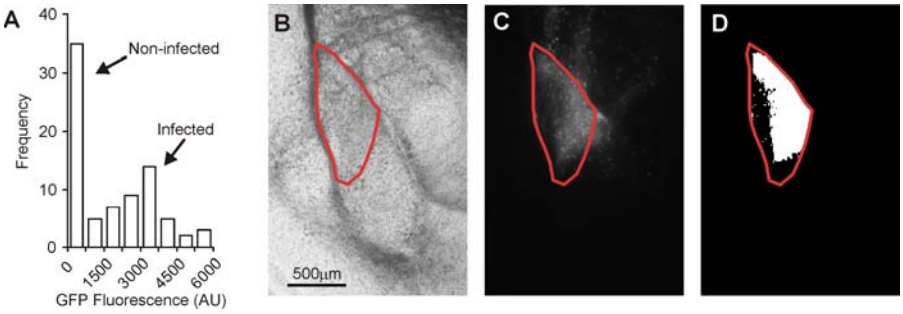

Fig. S2: Histological analysis of infection efficacy. (**A**) Distribution of green fluorescence intensities of neuronal somata identified in the red channel of double labelling experiments. The bimodal nature of the distribution indicates good discrimination of infected and non-infected neurons. (**B** and **C**) Lower magnification, transmitted light (B) and epifluorescence (C) images of same slice

as (Fig. 5B). Red line circumscribes lateral amygdala. (**D**) Estimation of infection size by thresholding of (C) (see methods for details).

References and Notes

S1. S. Shi, Y. Hayashi, J. A. Esteban, R. Malinow, *Cell* **105**, 331 (2001).

S2. F. Lim *et al.*, *Biotechniques* **20**, 460 (1996).

S3. W. A. Carlezon, Jr. *et al.*, *Science* **277**, 812 (1997).

S4. E. S. Faber, R. J. Callister, P. Sah, *J. Neurophysiol.* **85**, 714 (2001).

S5. J. E. LeDoux, *Annu. Rev. Neurosci.* **23**, 155 (2000).

S6. M. G. Weisskopf, E. P. Bauer, J. E. LeDoux, *J. Neurosci.* **19**, 10512 (1999).

S7. G. Paxinos, C. Watson, *The rat brain in stereotaxic coordinates* (Academic Press, San Diego, 1986).

S8. S. Maren, *Annu. Rev. Neurosci.* **24**, 897 (2001).